Solid State Communications 151 (2011) 272–275

Contents lists available at ScienceDirect

Solid State Communications

journal homepage: www.elsevier.com/locate/ssc

Effects of spin structures on Fermi surface topologies in $BaFe_2As_2$

Y. Wang [a,*], J.E. Saal [a], S.L. Shang [a], X.D. Hui [a,b], L.Q. Chen [a], Z.K. Liu [a]

[a] Department of Materials Science and Engineering, The Pennsylvania State University, University Park, PA 16802, USA

[b] State Key Laboratory for Advanced Metals and Materials, University of Science and Technology Beijing, Beijing 100083, China

ARTICLE INFO

Article history:
Received 28 May 2010
Received in revised form
10 November 2010
Accepted 7 December 2010
by Xianhui Chen
Available online 15 December 2010

Keywords:
A. Superconductors
A. Magnetically ordered materials
D. Fermi surface

ABSTRACT

The effects of spin structures on the Fermi surface topologies of $BaFe_2As_2$ were calculated using the first-principles approach. Here, we considered the nonmagnetic, Checkerboard, Stripe, and SDW (spin-density-wave) structures as well as a tetragonal structure labeled as STR17. By comparing the calculated results with the published angle-resolved photoemission spectroscopy from the literature, we propose that most of the experimentally observed Fermi surfaces of $BaFe_2As_2$ are the thermal mixture of those of the SDW, STR17, and Stripe structures.

It is commonly believed that the newly discovered iron arsenide superconductors [1] are possibly magnetically mediated [2]. However, being different from the cuprates where the parent compound is a Mott insulator, the parent compounds of the arsenide superconductors show a metallic behavior with a magnetically ordered state [3]. Hence, understanding the impact of magnetic ordering on the shapes of Fermi surface (FS), which is an abstract surface in momentum space separating the occupied from unoccupied states, may provide a way to investigate the mechanism of superconductivity in these materials. In this respect, $BaFe_2As_2$ is one of the most investigated parent compounds [3–8]. In particular, Singh [8] first reported the density functional calculation of the FS for $BaFe_2As_2$ assuming the nonmagnetic state and using the high temperature experimental tetragonal lattice parameters within the local density approximation (LDA) for the exchange–correlation potential; Ma et al. [6], using the experimental tetragonal crystal lattice parameters, calculated the FSs of the nonmagnetic state, the square antiferromagnetic Néel state (referred to as Checkerboard in this work), and the collinear antiferromagnetic state (referred to as spin-density-wave (SDW) state in this work) for $BaFe_2As_2$ under the generalized gradient approximation (GGA) of Perdew–Burke–Ernzerhof [9] for the exchange–correlation potential; Shimojima et al. [7], reported the measured FSs for $BaFe_2As_2$ below and above the Néel temperature and compared them with those obtained from LDA calculations using the experimental lattice constant.

In this work, we have made a more systematic first-principles study that details how magnetism affects the Fermi surface topology as a function of the spin structure. Unique from the previous work, which employed the experimental geometries, the present calculations use the theoretically fully optimized geometries. We report the calculated Fermi surface pockets for four spin structures and one nonmagnetic structure of the iron-based superconductor parent compound $BaFe_2As_2$. Fig. 1(a)–(e) illustrate the spin alignments of Fe atoms for the ordered (SDW) [6,10], STR17, Stripe [11,12], Checkerboard [6,11,12], and nonmagnetic (NM) [8] structures, respectively. Note that the structures plotted in Fig. 1(a)–(e) contain 2, 1, 2, 4, and 4 primitive unit cells, respectively. The spin structures of the Checkerboard, Stripe, and SDW are already known in the literature listed above.

We note that STR17 is a new magnetic structure proposed in this work, which is a superstructure achieved by rotating one of the two layers of Fe spins of the Stripe structure by 90°. When the spin symmetry is considered, its primitive unit cell contains 4 formula units. STR17 is unique due to its tetragonal symmetry (after the symmetry breaking due to the Fe spin configuration is neglected): a commonly observed symmetry for most of the iron arsenide superconductors [1,13–15]. STR17 could be a good candidate of an intermediate phase with broken symmetry (spuriously by spin distribution)—an important concept in understanding superconductivity [16].

The first-principles calculations are performed by employing the projector-augmented wave (PAW) method [17,18] within the generalized gradient approximation (GGA) of Perdew–Burke–Ernzerhof (PBE) [9] implemented in the VASP package [17,18]. A plane wave cutoff of 348.2 eV is used. Cell shape, cell volume,

* Corresponding author. Tel.: +1 814 863 9957.
E-mail address: yuw3@psu.edu (Y. Wang).

0038-1098/$ – see front matter © 2010 Elsevier Ltd. All rights reserved.
doi:10.1016/j.ssc.2010.12.012

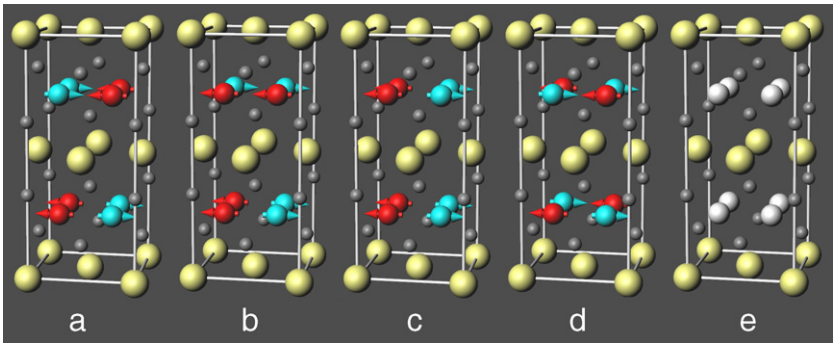

Fig. 1. (Color online). The magnetic structures of $BaFe_2As_2$ calculated in the current work: (a) SDW; (b) STR17; (c) Stripe; (d) Checkerboard; and (e) NM. Big golden spheres: Ba; Small grey spheres: As; Red spheres with arrows pointing left: Fe with spin up; Cyan spheres with arrows pointing right: Fe with spin down. Fe atoms are shown as white spheres for NM.

and atomic positions are all fully relaxed to find the equilibrium geometries for calculating the Fermi surfaces of the five structures.

Taking the total energy of the NM structure as the reference, the calculated total energies in the unit of the 20-atom supercell are −516.18, −497.29, −489.97, −122.65, and 0 meV, for the SDW, STR17, Stripe, Checkerboard, and NM structures, respectively. It therefore proves that the SDW structure is indeed the ground state, in agreement with experiments [19,20]. Note that the total energy for STR17 is lower, by −7.32 meV, than that of the Stripe, which is a prototype of many recent theoretical models [8,12,21]. Furthermore, the NM and Checkerboard structures are very high in energy when being compared with the Stripe, STR17, and SDW structures.

We now focus on the topologies of the FSs of $BaFe_2As_2$. Figs. 2 and 3 show the calculated FSs for the tetragonal structures and the orthorhombic structures, respectively. The 3D isosurfaces are plotted in Fig. 2(a) for NM, Fig. 2(b) for Checkerboard, Fig. 2(c) for STR17, Fig. 3(a) for Stripe, and Fig. 3(b) for SDW; the cuts at highly concentrated Fermi pockets are plotted in Fig. 2(d) for NM, Fig. 2(e), for Checkerboard, Fig. 2(f) for STR17, Fig. 3(b) for Stripe, and Fig. 3(d) for SDW; and top views of the isosurfaces are plotted in Fig. 2(g) for NM, Fig. 2(h) for Checkerboard, Fig. 2(i) for STR17, Fig. 3(e) for Stripe, and Fig. 3(f) for SDW.

Very recently, several experimental works based on angle-resolved photoemission spectroscopy (ARPES) were published in the literature. Kondo et al. [4] reported the measured FSs for pure $BaFe_2As_2$ at 20 K and 150 K. Liu et al. [5] reported the measured FSs for undoped and doped $BaFe_2As_2$ at 20 K, confirming the results of Kondo et al. that the X-pocket Fermi surface of the undoped samples resemble four flower petals. Yang et al. [22] reported the measured FSs for undoped $BaFe_2As_2$ in the paramagnetic state (tetragonal phase). In the above-mentioned three works, the experimental data were expressed in terms of the tetragonal symmetry, although the crystal structure of pure $BaFe_2As_2$ at 20 K is orthorhombic. The most elaborate experiment was from Shimojima et al. [7] who demonstrated that above T_N (Néel temperature), the observed FS showed a nearly circular shape with four-fold symmetry while below T_N, the FS obtained drastically split into a pair of relatively large FSs and a pair of small FSs (thus resulting in significantly modified FSs with two-fold symmetry).

From Fig. 2, it is seen that only the NM and Checkerboard structures consist of a double sheet hole-pocket (cyan area around the Z point in Fig. 2(d) for NM and small cyan area around the Z point in Fig. 2(e) for Checkerboard) and a double sheet electron-pocket (yellow area around the X point in Fig. 2(d) and (e)) although the majority of the Fermi pockets are single hole-packets (blue area just outside the double hole-pocket area in Fig. 2(d) and (e)) and single electron-pockets (red area just outside the double electron-pocket area in Fig. 2(d) and (e)).

For the NM structures, our calculated Fermi surfaces are identical to those calculated in previous works [8,12,21]. Specifically, the Γ (the symbol G is used to represent Γ in Figs. 2 and 3) points are two circle-like hole-pockets which are evolved and enlarged into round-corner squares at the Z point and around the X point are two ellipse-like electron-pockets. Interestingly, the measured FSs at the X point for the cobalt doped $Ba(Fe_{0.886}Co_{0.114})_2As_2$ by Liu et al. [5] (see Fig. 1(b) and (e) in the work published by Liu et al. [5]) are precisely reproduced by the present calculations for the NM and Checkerboard structures. However, we note that the NM and Checkerboard structures are much higher in energy compared to the Stripe, STR17, and SDW structures. Therefore, we advocate that, below the SDW ordering temperatures of 80–150 K [23–27], the NM and Checkerboard structures should be excluded from explaining the low temperature properties of undoped $BaFe_2As_2$ due to their high energies.

The SDW, STR17, and Stripe structures are stripe-based. Our calculations show that they consist of single sheet hole-pockets (small blue area between the Γ and Z points in Fig. 2(f) for STR17, blue area around the Γ point in Fig. 3(c) for Stripe, and small blue between the Γ and Z points in Fig. 3(d) for SDW) and single sheet electron-pockets (large red area just outside the single electron-pocket area in Fig. 2(f), red area around the Z point in Fig. 3(c), and red area around the Z point in Fig. 3(d)). The FSs of the STR17 structure (Fig. 2(c), (f) and (i)) are characterized by the circular electron-pocket with a square hole in the center in the $k_z = 0$ cut, the flower-like electron-pocket with four petals in the k_z = cut, and the small hole-pocket between the Γ and Z points. The FSs of the Stripe structure (Fig. 3(a), (c) and (e)) are characterized by a similar distorted flower-like electron-pocket along Z–T together with relatively small hole-pockets along Z-Γ. The FSs of the SDW structure (Fig. 3(b), (d) and (f)) contain two-fold electron-pockets along the Z–T direction together with rather small hole-pockets along Z-Γ. The calculated FSs for the Stripe structure and the SDW structure in Fig. 3 are greatly supported by the recent measurement by Shimojima et al. [7], as is demonstrated by the agreement between the calculation and the experiment concerning the shapes of the FSs near the Z points (compare Fig. 3 of this work with the measured data shown in Fig. 1(d) and (f) in the work published by Shimojima et al. [7]).

The calculated FSs for the STR17 structure shown in Fig. 2(c), (f) and (i) are especially interesting. Since the energy of the STR17 structure is even lower than that of Stripe, it could be substantially thermally populated even below T_N. Moreover, for $BaFe_2As_2$, we must realize that the experimentally observed high temperature tetragonal phase is paramagnetic. It is important to distinguish the paramagnetic and nonmagnetic phases [28]. In the paramagnetic phase, Fe atoms still possess local spin moments although completely disordered, while in the nonmagnetic phase there are no local spin moments at Fe sites. It could be assumed,

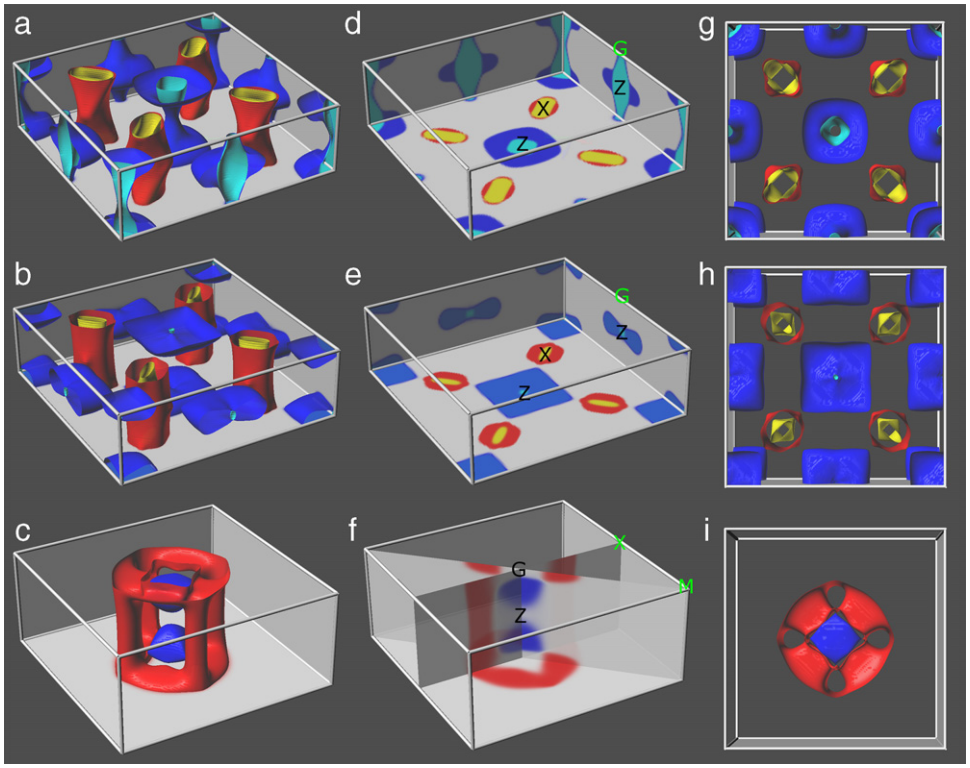

Fig. 2. (Color online). The calculated Fermi surfaces of tetragonal $BaFe_2As_2$. Isosurfaces: (a) NM; (b) Checkerboard; and (c) STR17. Cuts: (d) NM; (e) Checkerboard; and (f) STR17. Top views of isosurfaces: (g) NM; (h) Checkerboard; (i) STR17. The cyan, blue, red, and yellow colors have been used to mark the double sheet hole-pocket, single sheet hole-pocket, single sheet electron-pocket, and double sheet electron-pocket, respectively. The symbols G, Z, X, and M mark the high symmetry points in reciprocal space.

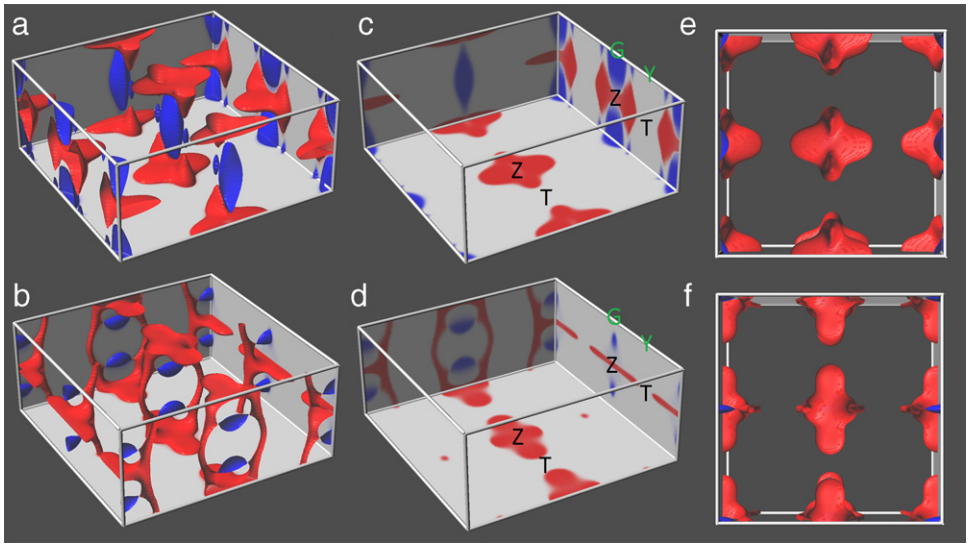

Fig. 3. (Color online). The calculated Fermi surfaces of orthorhombic $BaFe_2As_2$: Isosurfaces (a) Stripe and (b) SDW. Cuts: (c) Stripe and (d) SDW. Top views of isosurfaces: (e) Stripe and (f) SDW. The cyan, blue, red, and yellow colors have been used to mark the double sheet hole-pocket, single sheet hole-pocket, single sheet electron-pocket, and double sheet electron-pocket, respectively. The symbols G, Z, Y, and T mark the high symmetry points in reciprocal space.

therefore, that the STR17 structure can be substantially thermally populated above T_N. Indeed, the FSs as shown in Fig. 2(c), (f) and (i) of the STR17 structure show a trace of the four flower petals observed by Kondo et al. [4] (see Fig. 2(c1) and (c2) in the work published by Kondo et al. [4]) and by Liu et al. [5] (see Fig. 1(a) and (c) in the work published by Liu et al. [5]) and the circular shape with four-fold symmetry observed by Shimojima et al. [7] (see Fig. 1(d) and (e) in the work published by Shimojima et al. [7]) for the high temperature phase.

Since the total energies (in the unit of the 20-atom supercell, i.e., 4 formula units) of the STR17 and Stripe structures are just 18.89 and 26.21 meV higher, respectively, than that of the ground state SDW structure, the STR17 and Stripe structures should be substantially thermally occupied at around the $BaFe_2As_2$ SDW transition temperature in the range 80–150 K [23–27]. Therefore, we propose that most of the experimentally observed FSs of $BaFe_2As_2$ [4,5,21,22] (these experimental results are usually expressed in the form of tetragonal symmetry regardless of

temperature) are the thermal mixture of those of the SDW, STR17, and Stripe structures.

In summary, the effects of different spin structures on Fermi surface topologies of the iron-based superconductor parent compound $BaFe_2As_2$ have been calculated using the first-principles method. We have considered four magnetic structures: the observed low temperature ordered spin-density-wave (SDW) structure, the Checkerboard structure, the Stripe structure, and a 4 formula unit superstructure named STR17 proposed in the current work, together with the nonmagnetic structure. Since the calculated total energies of the STR17 and Stripe structures are rather close to that of the SDW structure, we propose that the experimentally observed Fermi surfaces of $BaFe_2As_2$ are the thermal mixture of those of the SDW, STR17, and Stripe structures at the $BaFe_2As_2$ SDW transition temperature around 80–150 K [23–27].

Acknowledgements

This work was funded by the Office of Naval Research (ONR) under contract No. N0014-07-1-0638, the National Science Foundation (NSF) through Grant No. DMR-1006557, and DOE Basic Sciences under Grant No. DOE DE-FG02-07ER46417 (Yi Wang and Chen), and in part supported by instrumentation funded by the National Science Foundation through grant OCI-0821527. Calculations were also conducted at the LION clusters at the Pennsylvania State University and at the National Energy Research Scientific Computing Center, which is supported by the Office of Science of the U.S. Department of Energy under Contract No. DE-AC02-05CH11231. This work was also supported in part by a grant of HPC resources from the Arctic Region Supercomputing Center at the University of Alaska Fairbanks as part of the Department of Defense High Performance Computing Modernization Program.

References

[1] Y. Kamihara, T. Watanabe, M. Hirano, H. Hosono, J. Am. Chem. Soc. 130 (2008) 3296.
[2] P. Monthoux, D. Pines, G.G. Lonzarich, Nature 450 (2007) 1177.
[3] H. Ding, P. Richard, K. Nakayama, K. Sugawara, T. Arakane, Y. Sekiba, A. Takayama, S. Souma, T. Sato, T. Takahashi, Z. Wang, X. Dai, Z. Fang, G.F. Chen, J.L. Luo, N.L. Wang, EPL 83 (2008) 47001.
[4] T. Kondo, R.M. Fernandes, R. Khasanov, C. Liu, A.D. Palczewski, N. Ni, M. Shi, A. Bostwick, E. Rotenberg, J. Schmalian, S.L. Bud'ko, P.C. Canfield, A. Kaminski, Phys. Rev. B 81 (2010) 060507.
[5] C. Liu, T. Kondo, R.M. Fernandes, A.D. Palczewski, E.D. Mun, N. Ni, A.N. Thaler, A. Bostwick, E. Rotenberg, J. Schmalian, S.L. Bud'ko, P.C. Canfield, A. Kaminski, Nat. Phys. 6 (2010) 419.
[6] F.J. Ma, Z.Y. Lu, T. Xiang, Front. Phys. China 5 (2010) 150.
[7] T. Shimojima, K. Ishizaka, Y. Ishida, N. Katayama, K. Ohgushi, T. Kiss, M. Okawa, T. Togashi, X.Y. Wang, C.T. Chen, S. Watanabe, R. Kadota, T. Oguchi, A. Chainani, S. Shin, Phys. Rev. Lett. 104 (2010) 057002.
[8] D.J. Singh, Phys. Rev. B 78 (2008) 094511.
[9] J.P. Perdew, K. Burke, M. Ernzerhof, Phys. Rev. Lett. 77 (1996) 3865.
[10] T. Yildirim, Phys. Rev. Lett. 102 (2009) 037003.
[11] J. Dong, H.J. Zhang, G. Xu, Z. Li, G. Li, W.Z. Hu, D. Wu, G.F. Chen, X. Dai, J.L. Luo, Z. Fang, N.L. Wang, EPL 83 (2008) 27006.
[12] G. Xu, H.J. Zhang, X. Dai, Z. Fang, EPL 84 (2008) 67015.
[13] R.J. McQueeney, S.O. Diallo, V.P. Antropov, G.D. Samolyuk, C. Broholm, N. Ni, S. Nandi, M. Yethiraj, J.L. Zarestky, J.J. Pulikkotil, A. Kreyssig, M.D. Lumsden, B.N. Harmon, P.C. Canfield, A.I. Goldman, Phys. Rev. Lett. 101 (2008) 227205.
[14] M.A. Tanatar, N. Ni, C. Martin, R.T. Gordon, H. Kim, V.G. Kogan, G.D. Samolyuk, S.L. Bud'ko, P.C. Canfield, R. Prozorov, Phys. Rev. B 79 (2009) 094507.
[15] J. Zhao, W. Ratcliff, J.W. Lynn, G.F. Chen, J.L. Luo, N.L. Wang, J.P. Hu, P.C. Dai, Phys. Rev. B 78 (2008) 140504.
[16] N. Doiron-Leyraud, C. Proust, D. LeBoeuf, J. Levallois, J.B. Bonnemaison, R.X. Liang, D.A. Bonn, W.N. Hardy, L. Taillefer, Nature 447 (2007) 565.
[17] P.E. Blöchl, Phys. Rev. B 50 (1994) 17953.
[18] G. Kresse, D. Joubert, Phys. Rev. B 59 (1999) 1758.
[19] C. de la Cruz, Q. Huang, J.W. Lynn, J.Y. Li, W. Ratcliff, J.L. Zarestky, H.A. Mook, G.F. Chen, J.L. Luo, N.L. Wang, P.C. Dai, Nature 453 (2008) 899.
[20] R.A. Ewings, T.G. Perring, R.I. Bewley, T. Guidi, M.J. Pitcher, D.R. Parker, S.J. Clarke, A.T. Boothroyd, Phys. Rev. B 78 (2008) 220501.
[21] C. Liu, G.D. Samolyuk, Y. Lee, N. Ni, T. Kondo, A.F. Santander-Syro, S.L. Bud'ko, J.L. McChesney, E. Rotenberg, T. Valla, A.V. Fedorov, P.C. Canfield, B.N. Harmon, A. Kaminski, Phys. Rev. Lett. 101 (2008) 177005.
[22] L.X. Yang, Y. Zhang, H.W. Ou, J.F. Zhao, D.W. Shen, B. Zhou, J. Wei, F. Chen, M. Xu, C. He, Y. Chen, Z.D. Wang, X.F. Wang, T. Wu, G. Wu, X.H. Chen, M. Arita, K. Shimada, M. Taniguchi, Z.Y. Lu, T. Xiang, D.L. Feng, Phys. Rev. Lett. 102 (2009) 107002.
[23] Q. Huang, Y. Qiu, W. Bao, M.A. Green, J.W. Lynn, Y.C. Gasparovic, T. Wu, G. Wu, X.H. Chen, Phys. Rev. Lett. 101 (2008) 257003.
[24] R. Mittal, Y. Su, S. Rols, T. Chatterji, S.L. Chaplot, H. Schober, M. Rotter, D. Johrendt, T. Brueckel, Phys. Rev. B 78 (2008) 104514.
[25] N. Ni, S.L. Bud'ko, A. Kreyssig, S. Nandi, G.E. Rustan, A.I. Goldman, S. Gupta, J.D. Corbett, A. Kracher, P.C. Canfield, Phys. Rev. B 78 (2008) 014507.
[26] M. Rotter, M. Tegel, D. Johrendt, Phys. Rev. Lett. 101 (2008) 107006.
[27] Y. Su, P. Link, A. Schneidewind, T. Wolf, P. Adelmann, Y. Xiao, M. Meven, R. Mittal, M. Rotter, D. Johrendt, T. Brueckel, M. Loewenhaupt, Phys. Rev. B 79 (2009) 064504.
[28] C. Kittel, Introduction to Solid State Physics, 8th ed., Wiley, Hoboken, NJ, 2005.